S. Simula
INFN - Roma Tre

XXXVIII International Symposium on
Lattice Field Theory
MIT, USA, July 26-30, 2021

Comparison of lattice QCD+QED predictions for radiative leptonic decays of light mesons with experimental data

in collaboration with:

R. Frezzotti, M. Garofalo, V. Lubicz, G. Martinelli, C.T. Sachrajda, F. Sanfilippo, N. Tantalo

Outline of the talk

* **leptonic decays of mesons** on the lattice using the RM123+Soton strategy [PRD '15 (1502.00257), PRL '18 (1711.06537), PRD '19 (1904.08731)]

* **real photon emission** on the lattice: structure-dependent form factors $F_V(E_\gamma)$ and $F_A(E_\gamma)$ [PRD '21 (2006.05358)]

* first-time comparison with **KLOE, E787, ISTRA+, OKA and PIBETA** experiments with **K and π** [PRD '21 (2012.02120)]

leptonic decays of PS mesons → extraction of CKM matrix elements

$$\Gamma(PS^+ \to \ell^+ \nu_\ell) = \frac{G_F^2}{8\pi} |V_{q_1 q_2}|^2 m_\ell^2 \left(1 - \frac{m_\ell^2}{m_{PS^+}^2}\right) M_{PS^+} f_{PS}^2 S_{ew} \left(1 + \delta R_{IB}^{PS} + \delta R_{QED}^{PS}\right)$$

S_{ew}: universal electroweak correction ($\simeq 1.032$)

f_{PS} : leptonic decay constant in isoQCD ($m_u = m_d$, $e_f = 0$)

δR_{IB}^{PS} : strong isospin breaking correction $\propto O[(m_d - m_u)/\Lambda_{QCD}] \simeq O(1\%)$

δR_{QED}^{PS} : QED correction $\propto O(\alpha_{em}) \simeq O(1\%)$

definition of isoQCD discussed in section 2 of arXiv:1904.08731

$$\left\{ M_{\pi^0}^{exp}, M_K^{FLAG}, M_{K^+}^{exp} - M_{K^0}^{exp}, M_{D_s}^{exp}, f_\pi^{PDG} \right\}$$

$\frac{f_K}{f_\pi}$: relative error of $\simeq 0.15\,\%$ FLAG-4 [EPJC '20]

* lattice determinations of f_{PS} have reached an accuracy below the percent level

need of determining δR_{IB}^{PS} and δR_{QED}^{PS} on the lattice

* **the infrared (IR) problem**: only $\Gamma(\Delta E_\gamma) = \Gamma_0 + \Gamma_1(\Delta E_\gamma)$ is IR finite [Block&Nordsiek '37] Γ_n : n photons in the final state

RM123+Soton strategy: $\Gamma(\Delta E_\gamma) = \lim_{V\to\infty}\left[\Gamma_0 - \Gamma_0^{pt}\right] + \lim_{V\to\infty}\left[\Gamma_0^{pt} + \Gamma_1(\Delta E_\gamma)\right]$ pt = point-like

IR finite IR finite

PRD '15 arXiv:1502.00257 (master formula)
PRD '17 arXiv:1611.08497 (FVEs)
PRL '18 arXiv:1711.06537 (π and K)
PRD '19 arXiv:1904.08731 (π and K)

$\lim_{V\to\infty}\left[\Gamma_0 - \Gamma_0^{pt}\right]$ on the lattice

$\lim_{m_\gamma\to 0}\left[\Gamma_0^{pt} + \Gamma_1^{pt}(\Delta E_\gamma)\right]$ within the pt approximation (small ΔE_γ)

large ΔE_γ → **real photon emission on the lattice** [PRD '21 arXiv:2006.05358]

non-perturbative hadronic amplitude

$$\epsilon^r_\mu(k)\ H^{\alpha\mu}_W(k,p) \equiv \epsilon^r_\mu(k) \int d^4y\ e^{iky} < 0\,|\,T\left[j^\alpha_W(0)\ j^\mu_{em}(y)\right]\,|\,PS(p) >$$

- $\epsilon^r_\mu(k)$: polarization vector of the photon with 4-momentum k
- $j^\alpha_W(0)$: weak current
- $j^\mu_{em}(y)$: em current
- $PS(p)$: PS meson with 4-momentum p

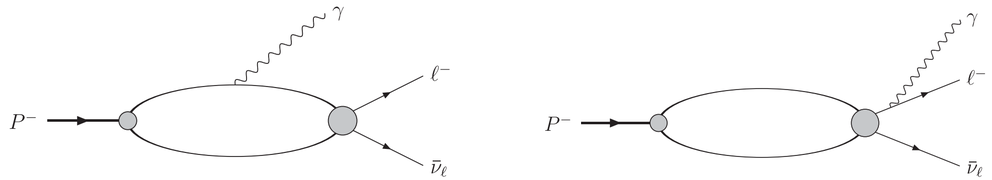

FIG. 1. Feynman diagrams representing the amplitudes with the emission of a real photon from the P^- meson (left panel) or from the final-state charged lepton ℓ^- (right panel).

four structure-dependent (dimensionless) form factors

see talk by F. Mazzetti (today, Hadron Structure)

$$H^{\alpha\mu}_W(k,p) = \frac{H_1}{m_{PS}}\left[k^2 g^{\alpha\mu} - k^\alpha k^\mu\right] + \frac{H_2}{m_{PS}}(p-k)^\alpha \frac{(p\cdot k - k^2)k^\mu - k^2(p-k)^\mu}{(p-k)^2 - m^2_{PS}}$$

H_1, H_2 : only for $k^2 \neq 0$

$$-i\frac{F_V}{m_{PS}}\epsilon^{\mu\alpha\beta\gamma}k_\beta p_\gamma + \frac{F_A}{m_{PS}}\left[(p\cdot k - k^2)g^{\alpha\mu} - k^\alpha (p-k)^\mu\right]$$

F_V, F_A : for both $k^2 = 0$ and $k^2 \neq 0$

$$+f_{PS}\left[g^{\alpha\mu} + \frac{(2p-k)^\mu (p-k)^\alpha}{2p\cdot k - k^2}\right]$$

pt (or Inner Bremsstrahlung) term (dictated by WI : $k_\mu H^{\alpha\mu}_W = f_{PS} p^\alpha$)

* here we consider only the case of real photon emission: $k^2 = 0$ and $\epsilon^r_\mu k^\mu = 0$

$$F_V = F_V(x_\gamma), \qquad F_A = F_A(x_\gamma) \qquad x_\gamma \equiv 2p\cdot k/m^2_{PS} = 2E_\gamma/m_{PS} \qquad \left(\vec{p}_{PS} = 0\right)$$

no IR divergent contribution in F_A

* F_V and F_A determined at the physical point for pion, kaon, D and D_s mesons

$$F^{\pm}(x_\gamma) \equiv F_V(x_\gamma) \pm F_A(x_\gamma)$$

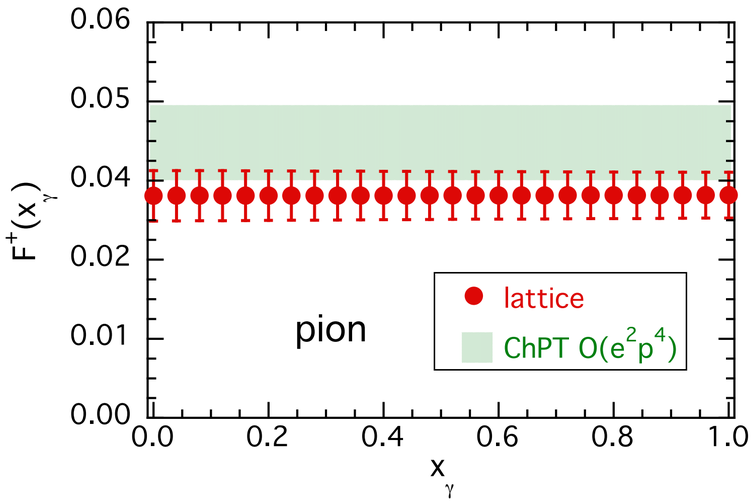

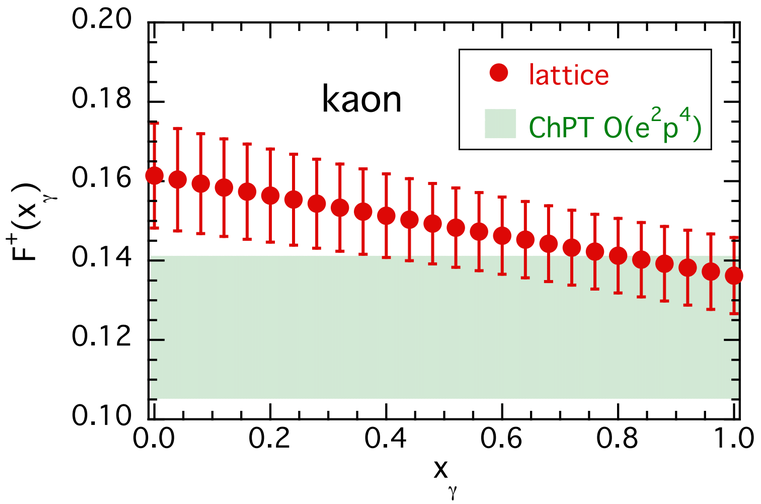

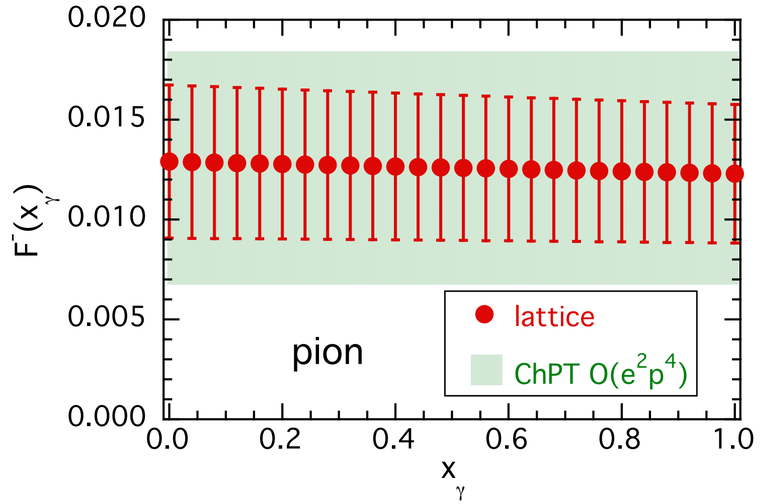

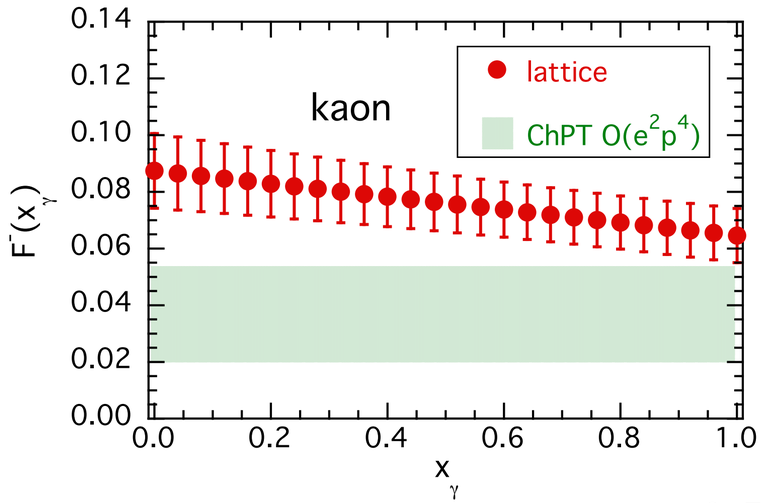

linear fit : $F^{\pm}(x_\gamma) = C^{\pm} + D^{\pm}\, x_\gamma$

mean values and covariance matrices
in PRD '21 arXiv:2012.02120

ChPT $O(e^2p^4)$: $F_V(x_\gamma) = \dfrac{m_{PS}}{4\pi^2 f_{PS}}$

$$F_A(x_\gamma) = \frac{8m_{PS}}{f_{PS}}\,(L_9^r + L_{10}^r)$$

$$L_9^r + L_{10}^r = 0.0017\ (7)$$

[Bijnens&Ecker '14]

$$x_\gamma \equiv 2p\cdot k/m_{PS}^2 = 2E_\gamma/m_{PS} \qquad (\vec{p}_{PS} = 0)$$

$$x_\ell \equiv 2p\cdot p_\ell/m_{PS}^2 = 2E_\ell/m_{PS}$$

$f_{\pm}^{SD,INT}$: kinematical terms

$$\Gamma(\Delta E_\gamma) = \Gamma^{(0)}\left[1 + \delta R_0 + \delta R_{pt}(\Delta E_\gamma) + \delta R_1^{SD}(\Delta E_\gamma) + \delta R_1^{INT}(\Delta E_\gamma)\right]$$

$$\frac{1}{\Gamma^{(0)}}\lim_{L\to\infty}\left[\Gamma_0(L) - \Gamma_0^{pt}(L)\right] \qquad \frac{1}{\Gamma^{(0)}}\lim_{m_\gamma\to 0}\left[\Gamma_0^{pt} + \Gamma_1^{pt}(\Delta E_\gamma)\right]$$

$$\delta R_1^{SD}(\Delta E_\gamma) = \int_0^{2\Delta E_\gamma/m_{PS}} dx_\gamma \int dx_\ell \left\{ f_+^{SD}(x_\gamma, x_\ell)\left[F^+(x_\gamma)\right]^2 + f_-^{SD}(x_\gamma, x_\ell)\left[F^-(x_\gamma)\right]^2 \right\}$$

$$\delta R_1^{INT}(\Delta E_\gamma) = \int_0^{2\Delta E_\gamma/m_{PS}} dx_\gamma \int dx_\ell \left\{ f_+^{INT}(x_\gamma, x_\ell)\ F^+(x_\gamma) + f_-^{INT}(x_\gamma, x_\ell)\ F^-(x_\gamma) \right\}$$

$$\Delta E_\gamma^{max} = \frac{m_{PS}}{2}\left(1 - \frac{m_\ell^2}{m_{PS}^2}\right)$$

inclusive leptonic decay rates

[PRD '21 arXiv:2012.02120]

$$\Gamma(\Delta E_\gamma^{max}) = \Gamma^{(0)}\left[1 + \delta R_0 + \delta R_{pt}(\Delta E_\gamma^{max}) + \delta R_1^{SD}(\Delta E_\gamma^{max}) + \delta R_1^{INT}(\Delta E_\gamma^{max})\right]$$

TABLE III. Values of the contributions δR_0, $\delta R_{\rm pt}(\Delta E_\gamma^{\rm max})$, $\delta R_1^{\rm SD}(\Delta E_\gamma^{\rm max})$ and $\delta R_1^{\rm INT}(\Delta E_\gamma^{\rm max})$, defined in Eqs. (35)-(38), evaluated using the lattice results of Refs. [7,8] for the decays $K(\pi) \to \mu(e)\nu[\gamma]$. In the last row the values of the maximum photon energy, $\Delta E_\gamma^{\rm max}$, are also shown for each decay process.

	$\pi_{e2[\gamma]}$	$\pi_{\mu 2[\gamma]}$	$K_{e2[\gamma]}$	$K_{\mu 2[\gamma]}$
δR_0	([a])	0.0411(19)	([a])	0.0341(10)
$\delta R_{\rm pt}(\Delta E_\gamma^{\rm max})$	−0.0651	−0.0258	−0.0695	−0.0317
$\delta R_1^{\rm SD}(\Delta E_\gamma^{\rm max})$	$5.4(1.0)\times 10^{-4}$	$2.6(5)\times 10^{-10}$	1.19(14)	$2.2(3)\times 10^{-5}$
$\delta R_1^{\rm INT}(\Delta E_\gamma^{\rm max})$	$-4.1(1.0)\times 10^{-5}$	$-1.3(1.5)\times 10^{-8}$	$-9.2(1.3)\times 10^{-4}$	$-6.1(1.1)\times 10^{-5}$
$\Delta E_\gamma^{\rm max}$ (MeV)	69.8	29.8	246.8	235.5

[a]Not yet evaluated by numerical lattice QCD + QED simulations. ← in progress

decays of π and K into muons and of π into electrons: negligible SD effects

decays of K into electrons: large SD effects → $\Gamma^0 \propto (m_\ell/m_{PS})^2$ (helicity suppression)

$\delta R_1^{SD} \propto (m_{PS}/m_\ell)^2$ (remove the suppression)

KLOE experiment $K \to e\nu_e\gamma$

[EPJC '09]

$$\Delta R^{exp,i} = \int_{E_\gamma^i}^{E_\gamma^{i+1}} dE_\gamma \, \frac{1}{\Gamma_{K\mu 2[\gamma]}} \left[\frac{d\Gamma(K_{e2\gamma})}{dE_\gamma} \right] \quad \to \quad \Delta R^{pt,i} + \Delta R^{SD,i} + \Delta R^{INT,i}$$

p_e>200 MeV (kinematical cut due to K_{e3} decays)

five bins : $E_\gamma^i = \{10, 50, 100, 150, 200, 250\}$ MeV

$E_\gamma^{max} \simeq 250$ MeV

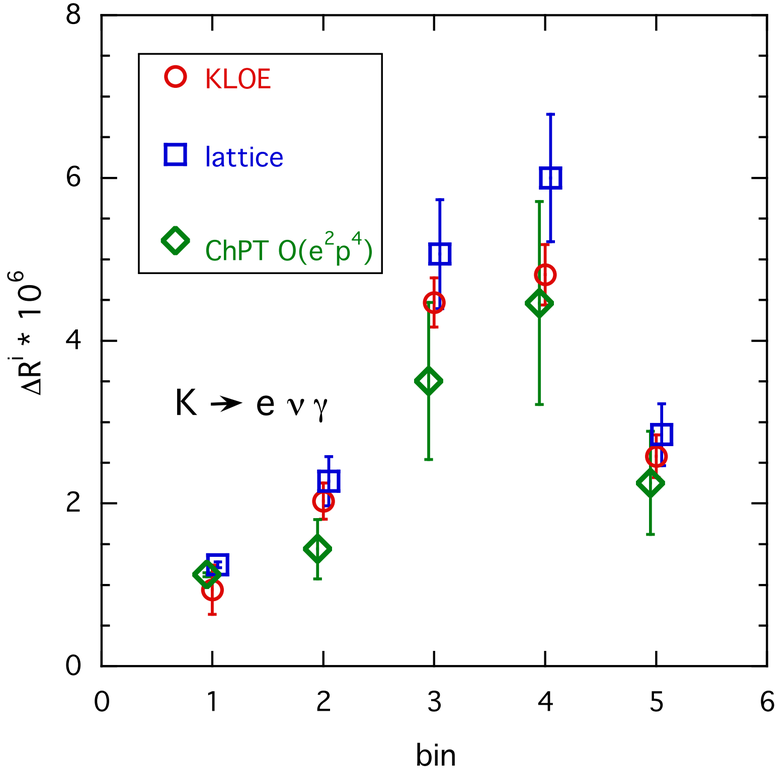

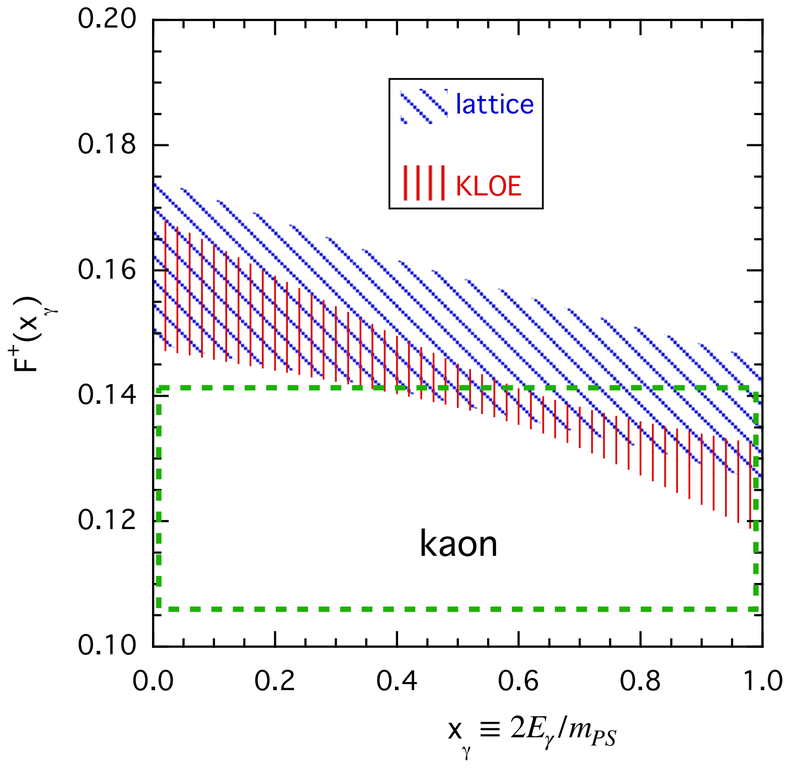

$\Delta R^{pt,i}$: relevant in the first bin only

$\Delta R^{INT,i}$: negligible

$$\Delta R^{SD,i} \propto \left[F_V(x_\gamma) + F_A(x_\gamma) \right]^2$$

ChPT $O(e^2p^4)$: $F_V(x_\gamma) = \dfrac{m_{PS}}{4\pi^2 f_{PS}}$

$$F_A(x_\gamma) = \frac{8m_{PS}}{f_{PS}} (L_9^r + L_{10}^r)$$

$$F^+(x_\gamma) = F_V(x_\gamma) + F_A(x_\gamma) \simeq 0.123 \pm 0.018$$

******* good consistency *******

FIG. 1. Left panel: comparison of the KLOE experimental data $\Delta R^{\mathrm{exp},i}$ [9] (red circles) with the theoretical predictions $\Delta R^{\mathrm{th},i}$, (blue squares) evaluated with the vector and axial form factors of Ref. [8] given in Eqs. (13)–(17), for the 5 bins (see Table IV). The green diamonds correspond to the prediction of ChPT at order $\mathcal{O}(e^2p^4)$, based on the vector and axial form factors given in Eq. (53). Right panel: comparison of the form-factor $F^+(x_\gamma)$ extracted by the KLOE collaboration in Ref. [9] and the theoretical prediction from Eqs. (13)–(17). The shaded areas represent uncertainties at the level of 1 standard deviation.

E787 experiment $K \to \mu\nu_\mu\gamma$

[PRL '00]

$$\frac{dR^{exp}}{d\cos(\theta_{\mu\gamma})} = \frac{1}{\Gamma_{K\mu2[\gamma]}} \left[\frac{d\Gamma(K_{\mu2\gamma})}{d\cos(\theta_{\mu\gamma})}\right]$$

E_γ>90 MeV, E_μ>243 MeV (kinematical cuts due to Kμ_3 decays)

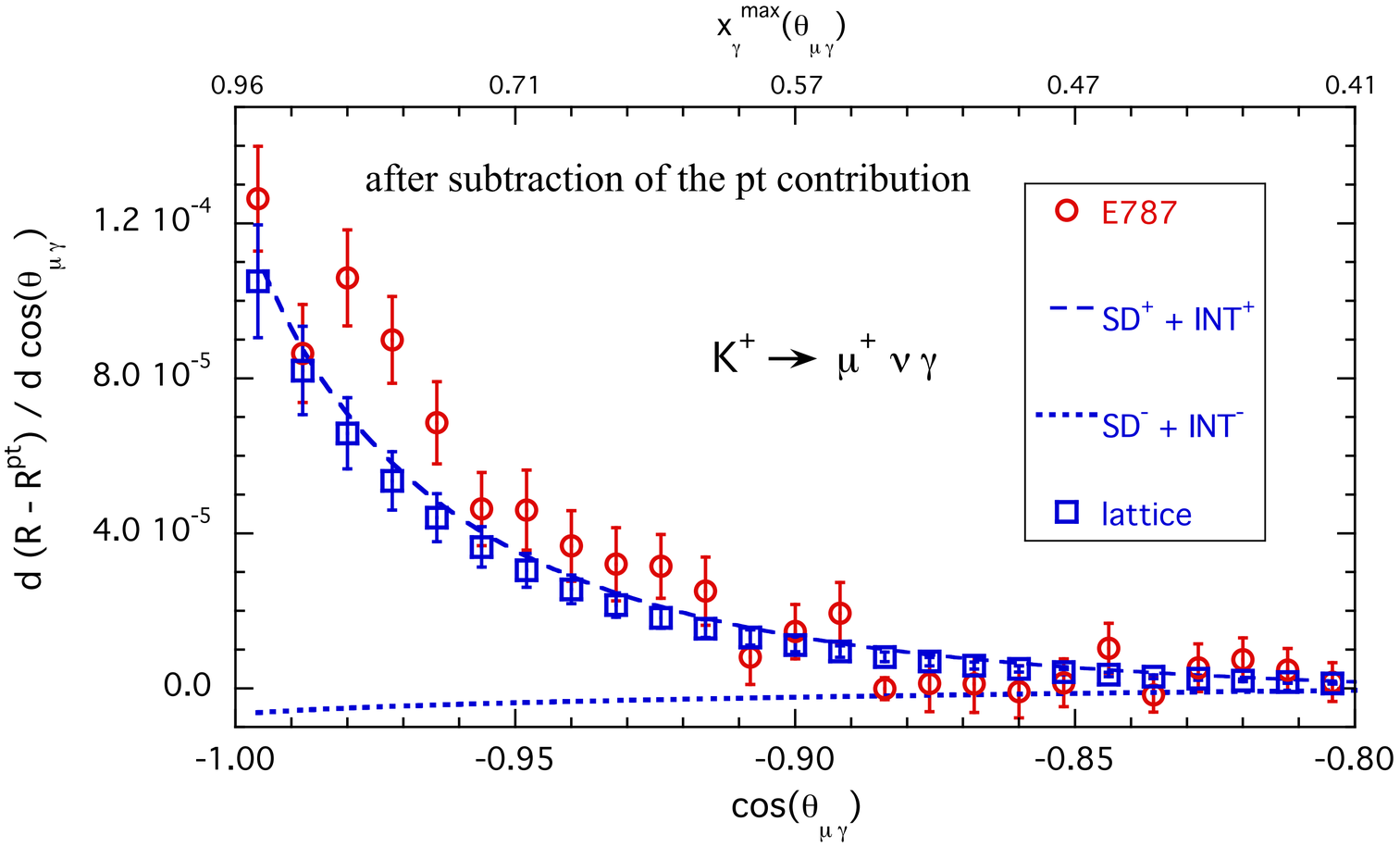

* tension at large backward angles (i.e. large x_γ) of about 2-3 standard deviations

$F^+(x_\gamma = 1) = 0.125 \pm 0.007_{\text{stat}} \pm 0.001_{\text{syst}}$ KLOE 2009

$F^+(x_\gamma = 1) = 0.165 \pm 0.007_{\text{stat}} \pm 0.011_{\text{syst}}$ E787 2000

difference of ~ 3 standard deviations at $x_\gamma = 1$

$F^+(x_\gamma = 1) = 0.136 \pm 0.010$ our work

forthcoming results from NA62 experiment on $K \to e\nu_e\gamma$

* opportunity for an accurate determination of $F^+(x_\gamma)$ in a wide range of values of x_γ (in particular for $x_\gamma \to 1$)

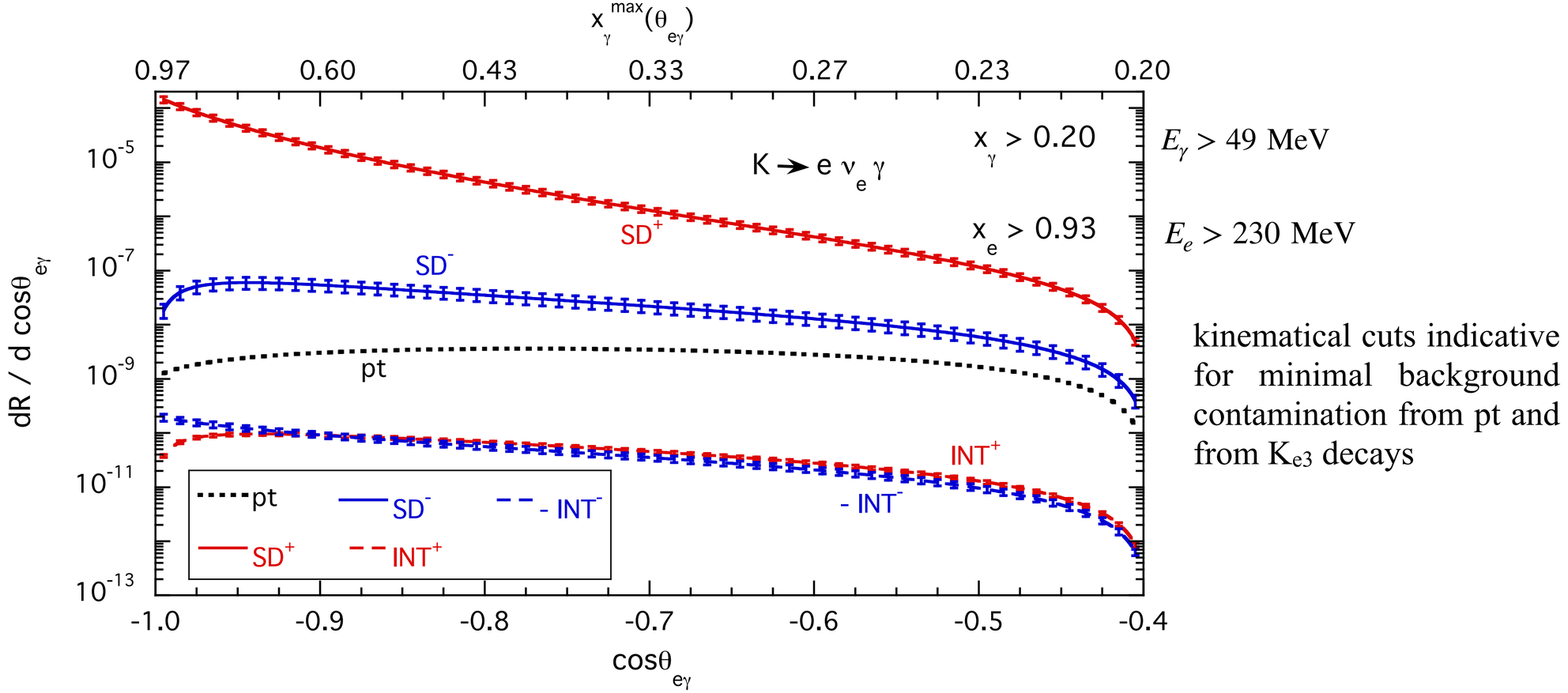

FIG. 3. Results for the pt, SD^+, SD^-, INT^+ and INT^- contributions to the differential branching ratio (57) as a function of the emission angle $\theta_{e\gamma}$ for the decay process $K_{e2\gamma}$, calculated using the lattice form factors of Ref. [8], given in Eqs. (13)–(17), with the kinematical cuts $x_\gamma > 0.2$ ($E_\gamma > 49$ MeV) and $x_e > 0.93$ ($E_e > 230$ MeV).

ISTRA+ and OKA experiments $K \to \mu\nu_\mu\gamma$

[PLB '11 and EPJC '19]

* kinematical cuts in the muon-photon angle $\theta_{\mu\gamma}$ and in the muon energy E_μ specific for each bin in x_γ in order to enhance the sensitivity to the INT contribution proportional to $F^-(x_\gamma) = F_V(x_\gamma) - F_A(x_\gamma)$

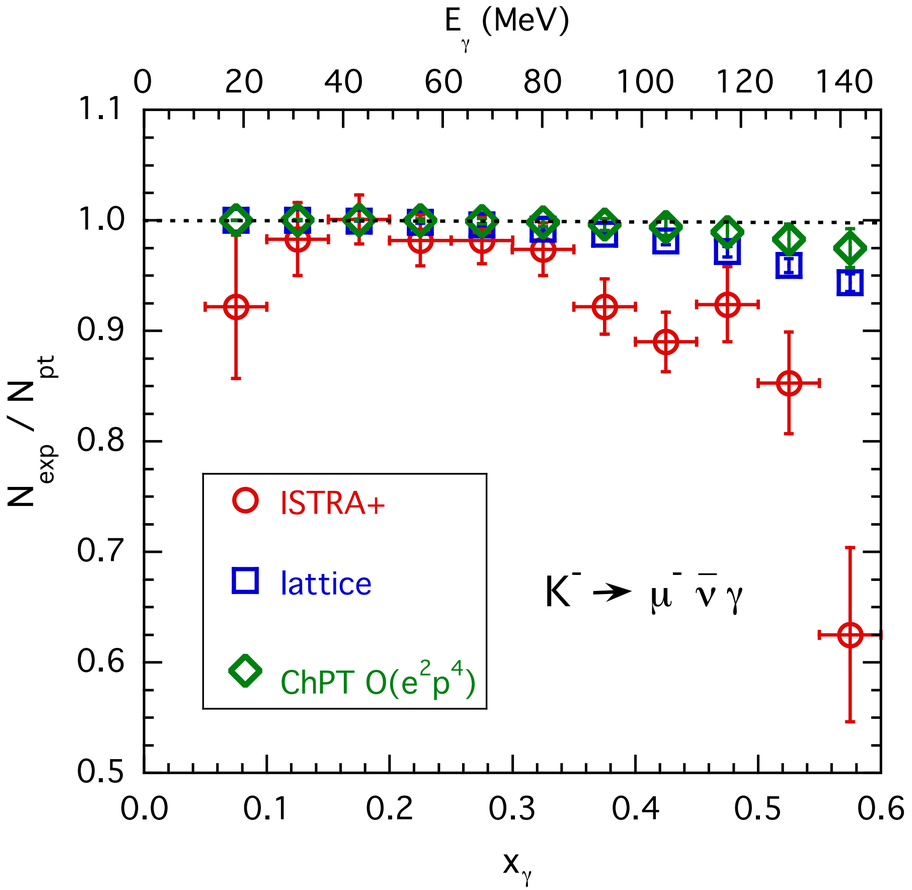

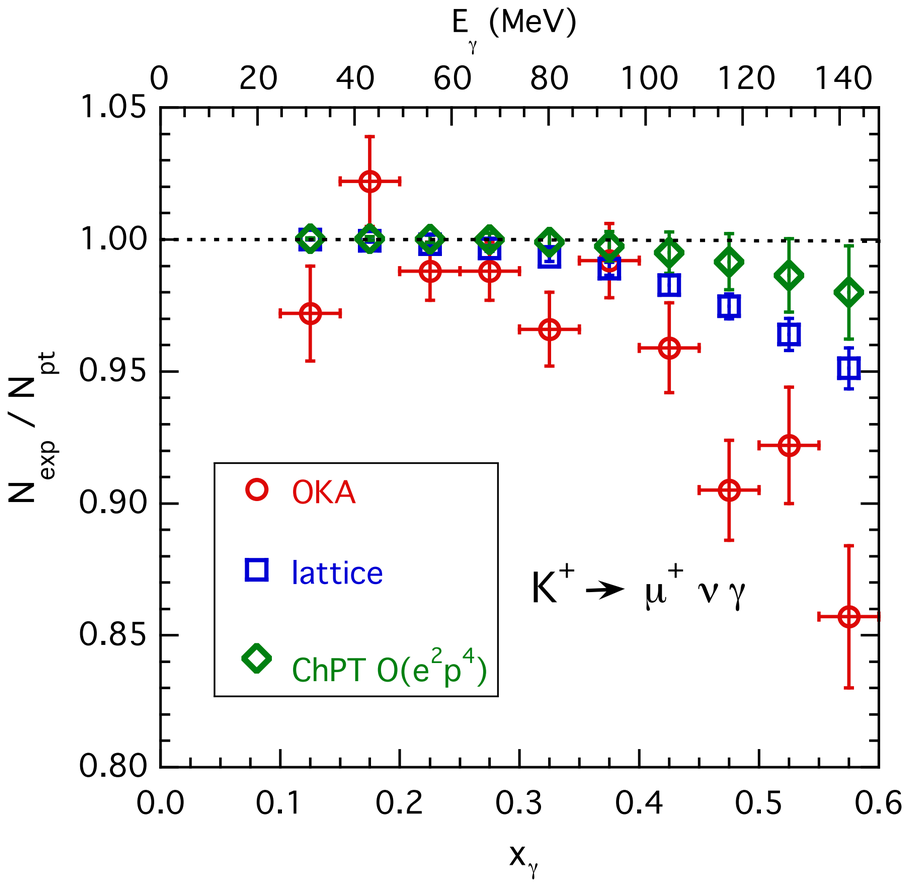

* discrepancies at large photon energies ($x_\gamma \gtrsim 0.5$): $\chi^2/(\mathrm{d.o.f.}) \simeq 3.9$ and 3.4 for ISTRA+ and OKA

PIBETA experiment $\pi \to e\nu_e\gamma$

[PRL '09]

$$\Delta R^{exp,i} = \frac{1}{\Gamma_{\pi e[\gamma]}} \int_{E_\gamma^i}^{E_\gamma^{max}} dE_\gamma \int_{E_e^i}^{E_e^{max}} \left[\frac{d^2\Gamma(K_{e2\gamma})}{dE_\gamma dE_e} \right]_{\theta_{e\gamma}>40^o}$$

four regions : $E_\gamma^i = \{50, 50, 10, 10\}$ MeV

$E_e^i = \{50, 10, 50, m_e\}$ MeV

$i = A, B, C, O$

$E_\gamma^{max} \simeq 70$ MeV

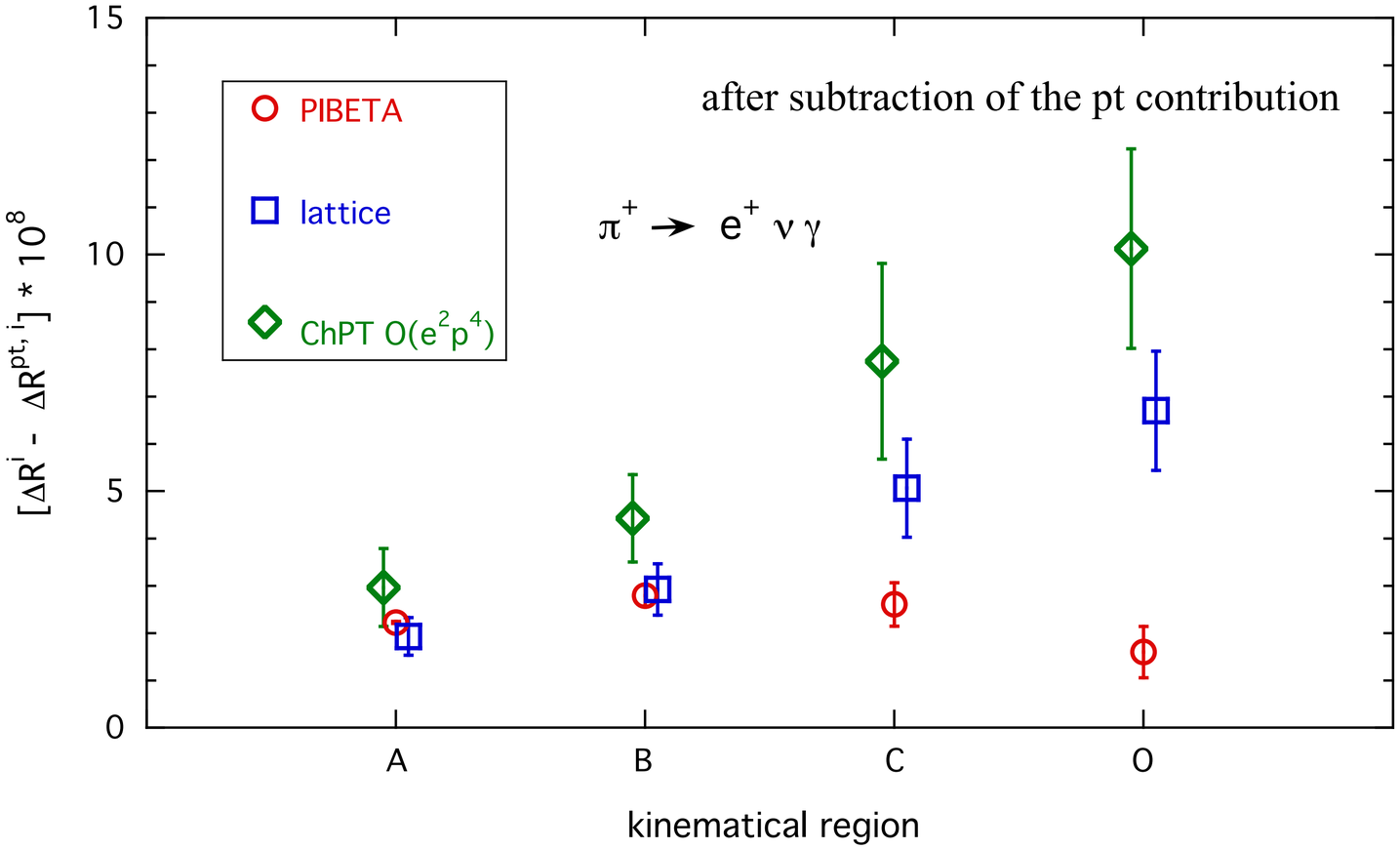

the cuts are basically more and more inclusive as one moves from A to O

$\Delta R^{INT,i}$: negligible

$\Delta R^{SD,i}$ increases from A to O

remarkable discrepancy
in the most inclusive region O

BSM: possible tensor interactions ?

Global SM fit of KLOE, E787, ISTRA+ and OKA data on $K \to \mu(e)\ \nu_{\mu(e)}\ \gamma$

linear fit : $F^{\pm}(x_\gamma) = C_\pm + D_\pm\ x_\gamma$ (d.o.f. = 51 - 4)

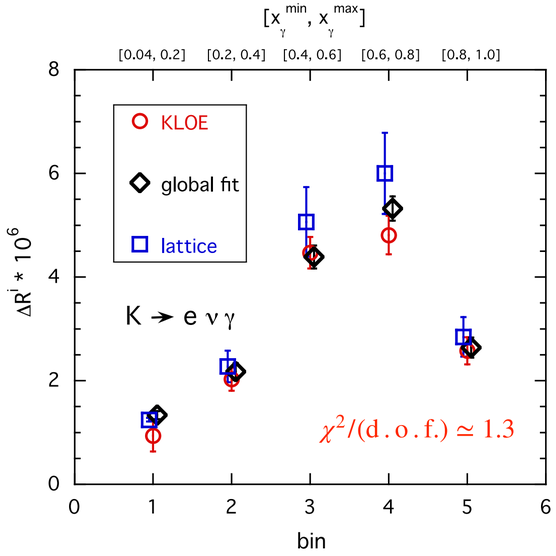

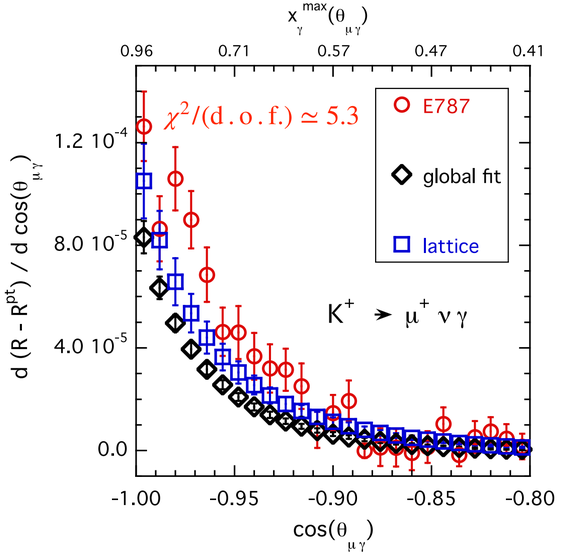

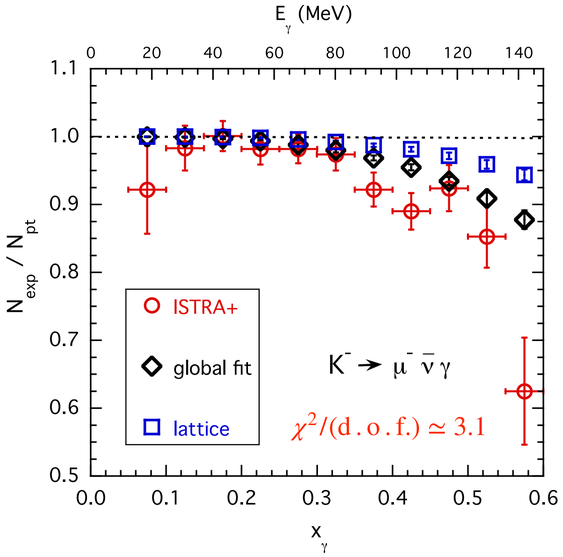

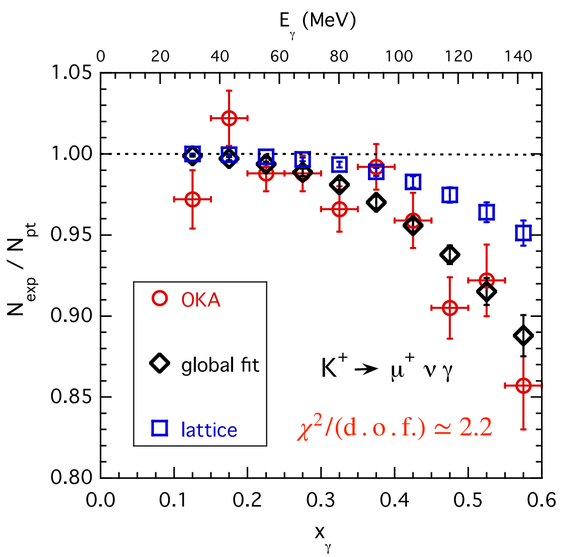

$C_+ = 0.134\ (12)$

$D_+ = -\ 0.002\ (19)$

$C_- = 0.157\ (49)$

$D_- = -\ 0.003\ (102)$

+ correlations

[arXiv: 2012.02120]

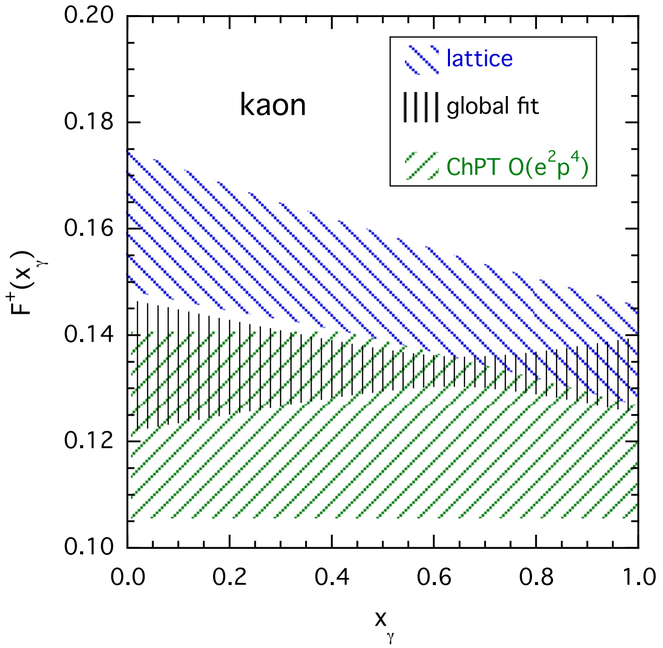

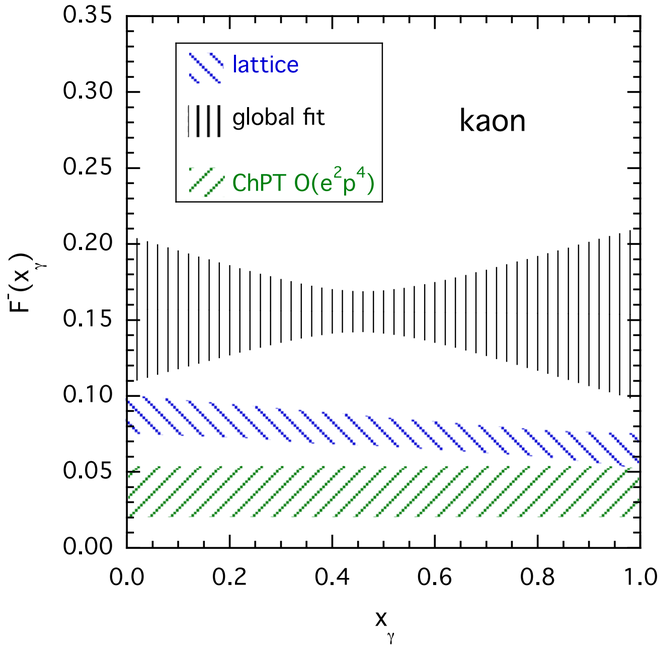

tension between KLOE ($\ell = e$) and E787 data ($\ell = \mu$) at large x_γ

* reasonable agreement with our $F^+(x_\gamma)$
* striking differences with our $F^-(x_\gamma)$

Conclusions

* first-time comparison of lattice QCD+QED predictions with data on $K \to e\nu_e\gamma$ from **KLOE**, on $K \to \mu\nu_\mu\gamma$ from **E787**, **ISTRA+** and **OKA**, on $\pi \to e\nu_e\gamma$ from **PIBETA** experiments

* **kaon**: good agreement with **KLOE** data ($\ell = e$), while a $\sim 2\sigma$ discrepancy for $F^+(x_\gamma)$ is visible at large x_γ with **E787** data ($\ell = \mu$)

* **kaon**: tension for $F^-(x_\gamma)$ at large x_γ with **ISTRA+** and **OKA** data

* **pion**: discrepancies in some kinematical regions of the **PIBETA** experiment

NA62 is expected to provide accurate results for $F^+(x_\gamma)$ from $K \to e\nu_e\gamma$

* global SM fit of **kaon** data from **KLOE**, **E787**, **ISTRA+** and **OKA**:
  - tension between KLOE and E787 at large x_γ
  - striking differences with our $F^-(x_\gamma)$ at large x_γ

need of improvements in the determination of the structure-dependent form factors from both experiment and theory

if confirmed, possible issues with flavor changing interactions beyond the SM V-A coupling and/or non-universal corrections to lepton couplings

ACK's:

B. Sciascia (KLOE) and T. Spadaro (KLOE, NA62)
M.R. Convery (E787)
M. Bychkov (PIBETA)
V. Kratsov, V. Duk and V. Obraztsov (OKA)
A. Romano (NA62)

backup slides

ETMC gauge configurations

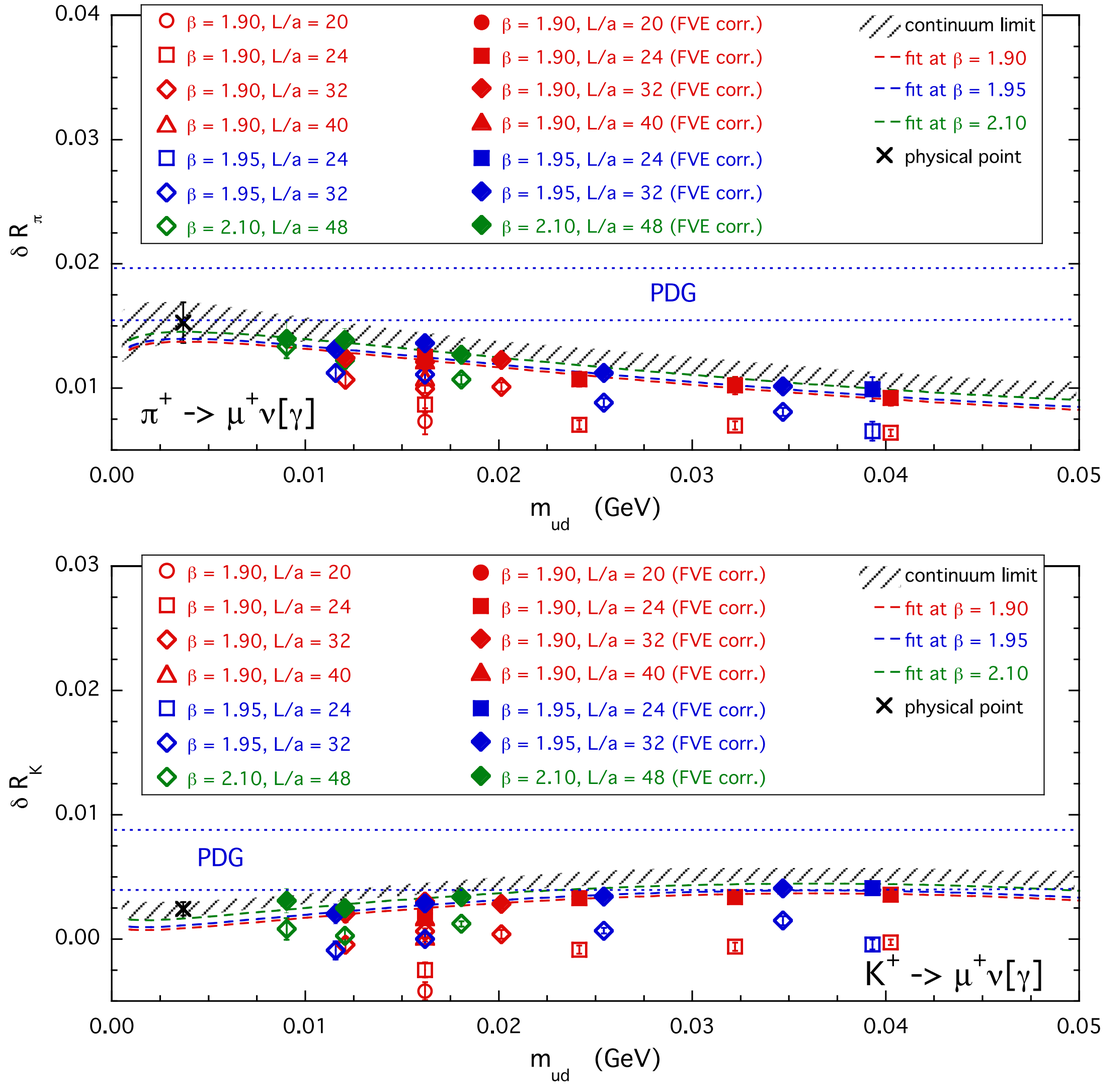

FIG. 10. Results for the corrections δR_π (top panel) and δR_K (bottom panel) obtained after the subtraction of the "universal" FSE terms up to order $\mathcal{O}(1/L)$ in Eq. (95) (empty markers). The full markers correspond to the lattice data corrected by the residual FSEs obtained in the case of the fitting function (98) including the chiral log. The dashed lines are the (central) results in the infinite volume limit at each value of the lattice spacing, while the shaded areas identify the results in the continuum limit at the level of 1 standard deviation. The crosses represent the values $\delta R_\pi^{\rm phys}$ and $\delta R_K^{\rm phys}$ extrapolated at the physical point $m_{ud}^{\rm phys}(\overline{\rm MS}, 2\ {\rm GeV}) = 3.70(17)$ MeV [28]. The blue dotted lines correspond to the values $\delta R_\pi^{\rm phys} = 0.0176(21)$ and $\delta R_K^{\rm phys} = 0.0064(24)$, obtained using ChPT [25] and adopted by the PDG [26].

PRD '19 arXiv:1904.08731

$$\Gamma(PS^+ \to \ell^+ \nu_\ell[\gamma]) = \frac{G_F^2}{8\pi} |V_{q_1 q_2}|^2 m_\ell^2 \left(1 - \frac{m_\ell^2}{m_{PS^+}^2}\right) M_{PS^+} f_{PS}^2 S_{ew} \left(1 + \delta R_{PS}\right)$$

$$\begin{aligned} \delta R_\pi^{\rm phys} &= +0.0153(16)_{\rm stat+fit}(4)_{\rm input}(3)_{\rm chiral} \\ &\quad \times (6)_{\rm FVE}(2)_{\rm disc}(6)_{q\rm QED} \\ &= +0.0153(19), \end{aligned} \tag{101}$$

$$\begin{aligned} \delta R_K^{\rm phys} &= +0.0024(6)_{\rm stat+fit}(3)_{\rm input}(1)_{\rm chiral}(3)_{\rm FVE}(2)_{\rm disc} \\ &\quad \times (6)_{q\rm QED} \\ &= +0.0024(10), \end{aligned} \tag{102}$$

$$\delta R_{K\pi}^{\rm phys} = \delta R_K^{\rm phys} - \delta R_\pi^{\rm phys} = -0.0126(14). \tag{106}$$

real photon emission on the lattice

[PRD '21 arXiv:2006.05358]

$$C^{\alpha r}(t;\vec{k},\vec{p}) = -i\epsilon^r_\mu(k)\int d^4y d^3x\; e^{t_y E_\gamma - i\vec{k}\cdot\vec{y}+i\vec{p}\cdot\vec{x}} < 0\,|\,T\left[j^\alpha_W(t)\; j^\mu_{em}(y)\; PS(0,\vec{x})\right]\,|\,0>$$

photon momentum — meson momentum — $E_\gamma = |\vec{k}|$ — weak current at t — em current — interpolating PS field at t_x=0

analytic continuation OK: intermediate states heavier than the external one $\sqrt{m^2_{PS}+|\vec{p}-\vec{k}|^2}+|\vec{k}| > E_{PS} = \sqrt{m^2_{PS}+|\vec{p}|^2}$ for $|\vec{k}| \neq 0$

$$\lim_{t\to\infty}\frac{2E_{PS}}{e^{-t(E_{PS}-E_\gamma)} < 0\,|\,PS(0)\,|\,PS(\vec{p})>} C^{\alpha r}(t;\vec{k},\vec{p}) = \epsilon^r_\mu(k)\; H^{\alpha\mu}_W(k,p)$$

care should be taken in the axial case: possible IR divergent discretization effects due to the subtraction of the pt contribution

matrix element $\propto x_\gamma F_A(x_\gamma) + 2\frac{f_{PS}}{m_{PS}}$ ➡ $O\left(\frac{a^2}{x_\gamma}\right)$ in $F_A(x_\gamma)$

subtraction of the matrix element at $x_\gamma = 0$

no IR divergent contribution in F_A

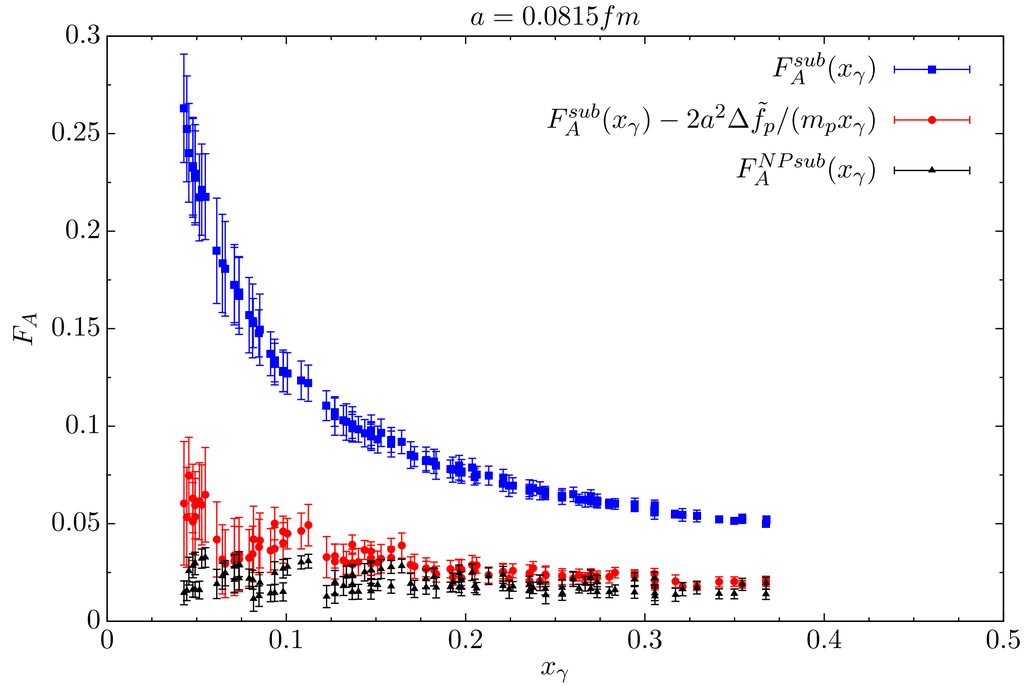

plateaux

vector case

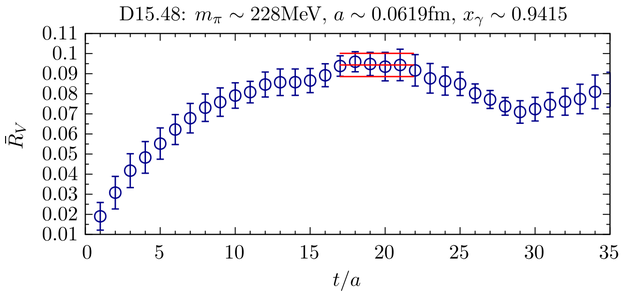

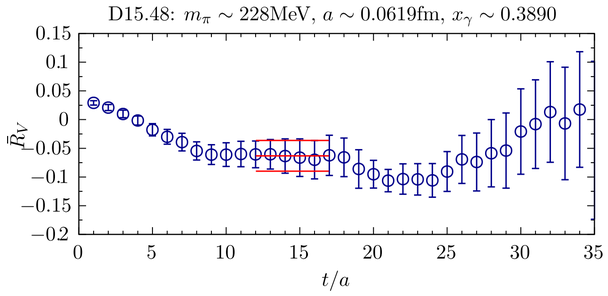

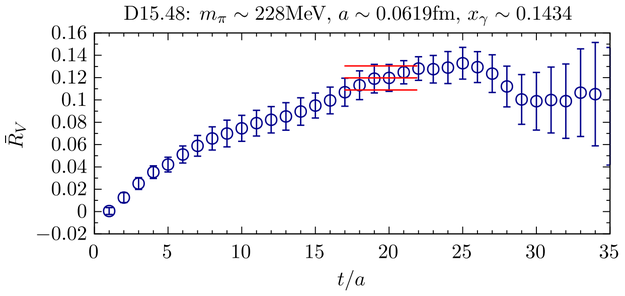

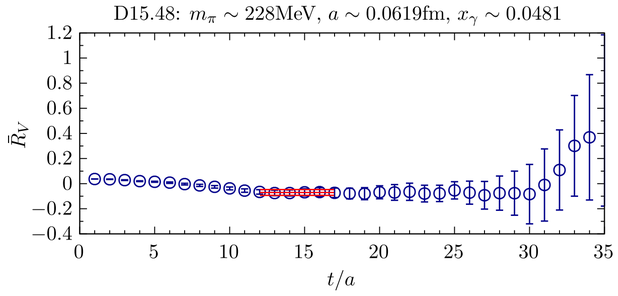

axial case

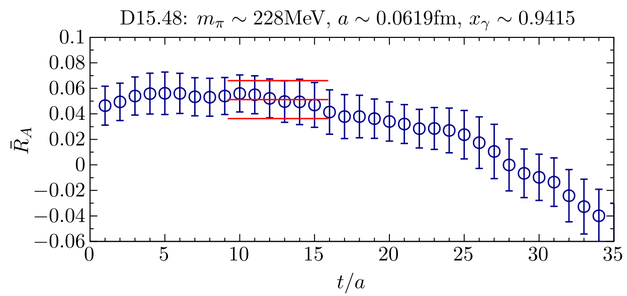

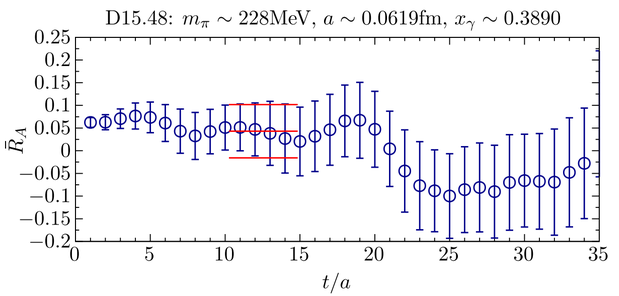

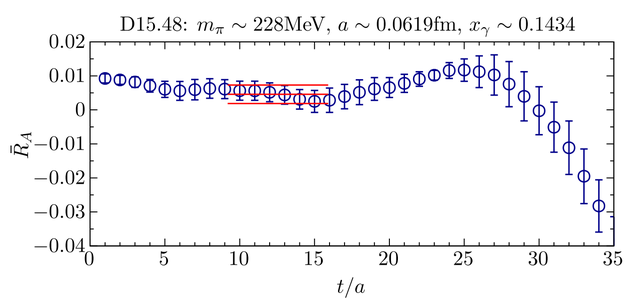

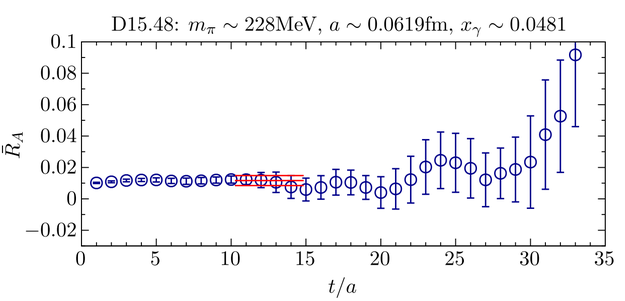

pion mass and a² dependencies

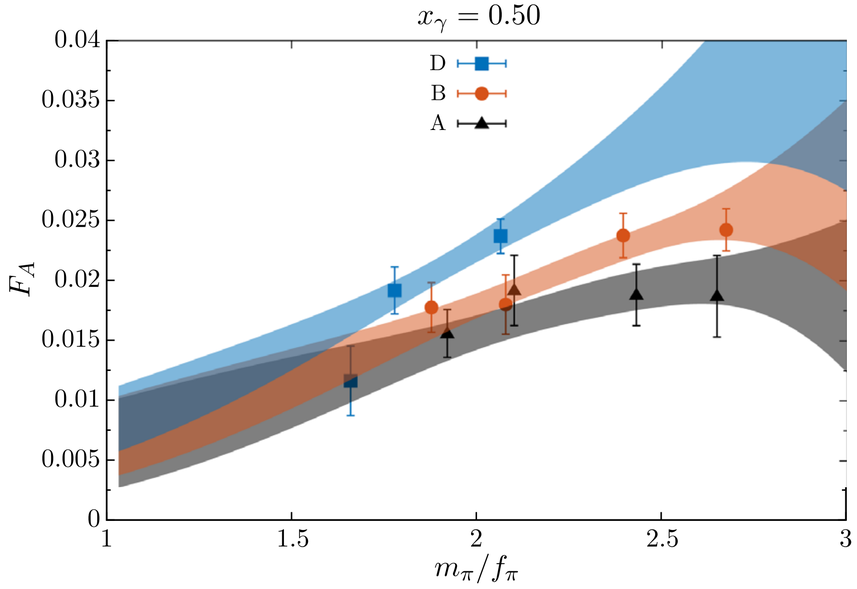

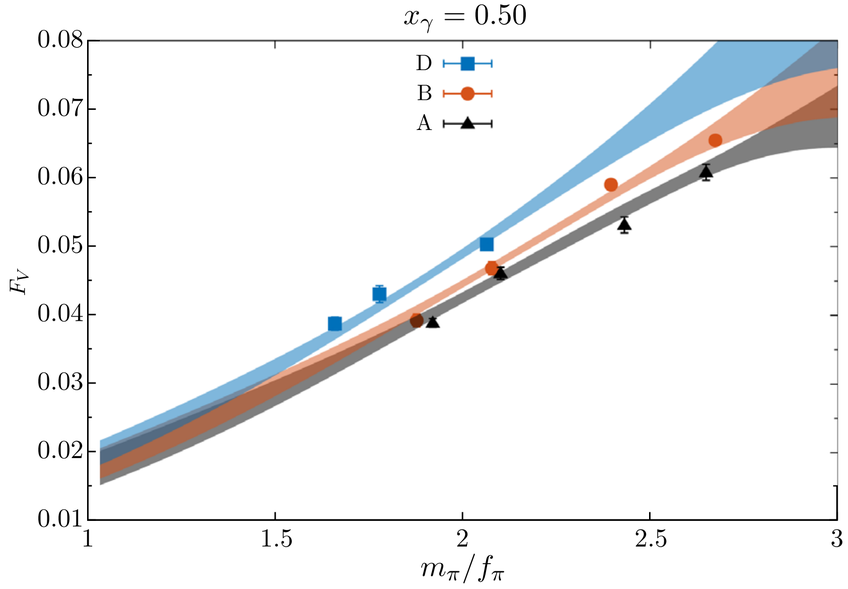

F_V and F_A determined at the physical point for pion, kaon, D and D_s mesons

KLOE experiment $K \to e\nu_e\gamma$

TABLE IV. Values of the KLOE experimental data $\Delta R^{\mathrm{exp},i}$ [9] and of the theoretical predictions $\Delta R^{\mathrm{SD},i}$ and $\Delta R^{\mathrm{th},i}$, evaluated with the vector and axial form factors of Ref. [8] given in Eqs. (13)–(17), tabulated in the 5 bins of the photon's energy adopted by the KLOE experiment on $K \to e\nu\gamma$ decays. The seventh column is the ratio between the experimental data and our theoretical predictions. In the fourth column the first error is statistical and the second one is systematic. The last column shows the prediction of ChPT at order $\mathcal{O}(e^2p^4)$, based on the vector and axial form factors given in Eq. (53).

Bin	E_γ (MeV)	p_e (MeV)	$\Delta R^{\mathrm{exp},i} \times 10^6$	$\Delta R^{\mathrm{SD},i} \times 10^6$	$\Delta R^{\mathrm{th},i} \times 10^6$	exp / th	ChPT
1	10–50	> 200	$0.94 \pm 0.30 \pm 0.03$	0.26 ± 0.04	1.25 ± 0.04	0.75 ± 0.24	1.13 ± 0.03
2	50–100	> 200	$2.03 \pm 0.22 \pm 0.02$	2.26 ± 0.30	2.28 ± 0.30	0.89 ± 0.15	1.44 ± 0.36
3	100–150	> 200	$4.47 \pm 0.30 \pm 0.03$	5.06 ± 0.67	5.07 ± 0.67	0.88 ± 0.13	3.50 ± 0.96
4	150–200	> 200	$4.81 \pm 0.37 \pm 0.04$	6.00 ± 0.78	6.00 ± 0.78	0.80 ± 0.12	4.46 ± 1.25
5	200–250	> 200	$2.58 \pm 0.26 \pm 0.03$	2.85 ± 0.38	2.85 ± 0.38	0.91 ± 0.15	2.25 ± 0.63
1–5	10–250	> 200	$14.83 \pm 0.66 \pm 0.13$	16.43 ± 2.12	17.43 ± 2.12	0.85 ± 0.11	12.79 ± 3.24

ISTRA+ and OKA experiments $K \to \mu\nu_\mu\gamma$

TABLE VI. Kinematical cuts adopted in the ISTRA+ experiment of Ref. [11] (see text).

Strip	x_γ	y_μ	$\cos(\theta_{\rm cut})$
01	$0.05 < x_\gamma < 0.10$	$0.90 < y_\mu < 1.10$	−0.8
02	$0.10 < x_\gamma < 0.15$	$0.90 < y_\mu < 1.10$	−0.8
03	$0.15 < x_\gamma < 0.20$	$0.85 < y_\mu < 1.00$	−0.8
04	$0.20 < x_\gamma < 0.25$	$0.80 < y_\mu < 0.95$	−0.2
05	$0.25 < x_\gamma < 0.30$	$0.75 < y_\mu < 0.90$	−0.3
06	$0.30 < x_\gamma < 0.35$	$0.72 < y_\mu < 0.87$	−0.4
07	$0.35 < x_\gamma < 0.40$	$0.65 < y_\mu < 0.85$	−0.3
08	$0.40 < x_\gamma < 0.45$	$0.62 < y_\mu < 0.85$	−0.5
09	$0.45 < x_\gamma < 0.50$	$0.57 < y_\mu < 0.80$	−0.7
10	$0.50 < x_\gamma < 0.55$	$0.52 < y_\mu < 0.75$	−1.0
11	$0.55 < x_\gamma < 0.60$	$0.48 < y_\mu < 0.70$	−1.0

TABLE VII. The same as in Table VI, but in the case of the OKA experiment of Ref. [12].

Strip	x_γ	y_μ	$\cos(\theta_{\rm cut})$
01	$0.10 < x_\gamma < 0.15$	$0.89 < y_\mu < 1.01$	−0.8
02	$0.15 < x_\gamma < 0.20$	$0.85 < y_\mu < 1.01$	−0.2
03	$0.20 < x_\gamma < 0.25$	$0.80 < y_\mu < 1.00$	−0.2
04	$0.25 < x_\gamma < 0.30$	$0.75 < y_\mu < 0.97$	−0.4
05	$0.30 < x_\gamma < 0.35$	$0.70 < y_\mu < 0.93$	−0.4
06	$0.35 < x_\gamma < 0.40$	$0.66 < y_\mu < 0.90$	−0.5
07	$0.40 < x_\gamma < 0.45$	$0.62 < y_\mu < 0.88$	−0.5
08	$0.45 < x_\gamma < 0.50$	$0.58 < y_\mu < 0.86$	−0.6
09	$0.50 < x_\gamma < 0.55$	$0.54 < y_\mu < 0.83$	−0.6
10	$0.55 < x_\gamma < 0.60$	$0.50 < y_\mu < 0.80$	−0.6

PIBETA experiment $\pi \to e\nu_e\gamma$

TABLE IX. Values of the PIBETA experimental results $\Delta R^{\mathrm{exp},i}$ [13], of the pt contribution $\Delta R^{\mathrm{pt},i}$, of the quantity $(\Delta R^{\mathrm{exp},i} - \Delta R^{\mathrm{pt},i})$ and of the theoretical predictions $\Delta R^{\mathrm{SD},i}$ and $(\Delta R^{\mathrm{th},i} - \Delta R^{\mathrm{pt},i})$, evaluated with the vector and axial form factors of Ref. [8] given in Eqs. (13)–(17), corresponding to the four kinematical regions adopted in the PIBETA experiment on $\pi^+ \to e^+\nu\gamma$ decays. Energies and branching ratios are given in units of MeV and 10^{-8}, respectively. In the kinematical region A the constraint $\theta_{e\gamma} > 40^\circ$ is automatically satisfied [13]. The last column shows the prediction of ChPT at order $\mathcal{O}(e^2p^4)$, based on the vector and axial form factors given in Eq. (53).

Region	E_γ	E_e	$\theta_{e\gamma}$	$\Delta R^{\mathrm{exp},i}$	$\Delta R^{\mathrm{pt},i}$	$(\Delta R^{\mathrm{exp},i} - \Delta R^{\mathrm{pt},i})$	$\Delta R^{\mathrm{SD},i}$	$(\Delta R^{\mathrm{th},i} - \Delta R^{\mathrm{pt},i})$	ChPT
A	> 50	> 50	$> 40^\circ$	2.614 ± 0.021	0.385	2.229 ± 0.021	1.94 ± 0.40	1.93 ± 0.40	2.97 ± 0.82
B	> 50	> 10	$> 40^\circ$	14.46 ± 0.22	11.66	2.80 ± 0.22	3.01 ± 0.54	2.93 ± 0.54	4.43 ± 0.92
C	> 10	> 50	$> 40^\circ$	37.69 ± 0.46	35.08	2.61 ± 0.46	5.07 ± 1.03	5.07 ± 1.04	7.75 ± 2.07
O	> 10	$> m_e$	$> 40^\circ$	73.86 ± 0.54	72.26	1.60 ± 0.54	6.87 ± 1.26	6.70 ± 1.26	10.13 ± 2.11

Global fit of KLOE, E787, ISTRA+ and OKA data on $K \to \mu(e)\ \nu_{\mu(e)}\ \gamma$

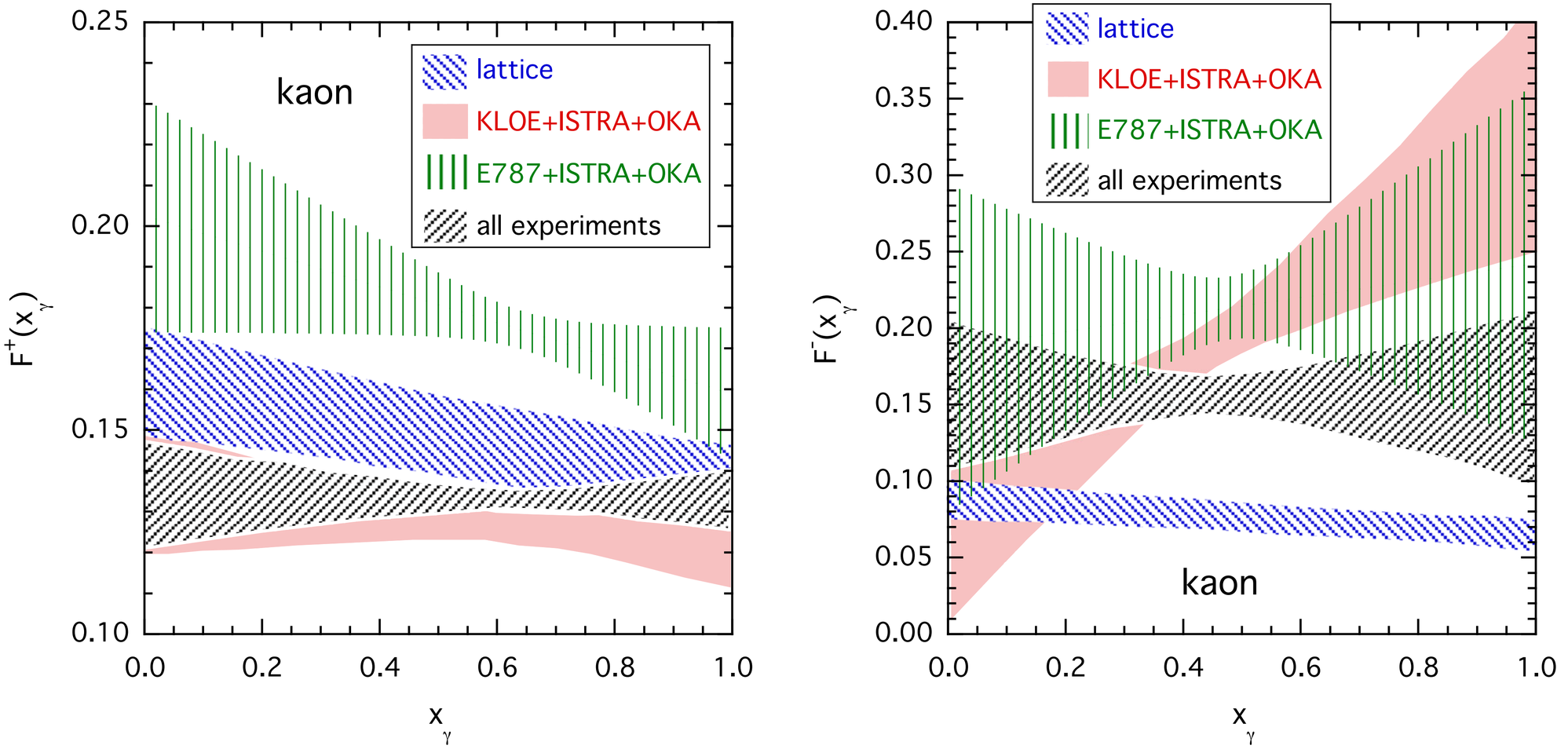

FIG. 8. Comparison of the form factors $F^+(x_\gamma)$ (left panel) and $F^-(x_\gamma)$ (right panel), given in Eq. (71), obtained by the fitting either KLOE [9], ISTRA+ [11] and OKA [12] data (red shaded areas) or E787 [10], ISTRA+ [11] and OKA [12] data (green shaded areas). The black shaded areas correspond to the simultaneous fit of all the experimental data from KLOE [9], E787 [10], ISTRA+ [11] and OKA [12]. The blue shaded areas represent our lattice results from Ref. [8]. All the shaded areas represent uncertainties at the level of 1 standard deviation.